Journal of Biotechnology 233 (2016) 171–180

Contents lists available at ScienceDirect

Journal of Biotechnology

journal homepage: www.elsevier.com/locate/jbiotec

High-efficiency transduction and specific expression of ChR2opt for optogenetic manipulation of primary cortical neurons mediated by recombinant adeno-associated viruses

Lei Jin[a], Wienke Lange[a], Annika Kempmann[b], Vanessa Maybeck[a,*], Anne Günther[b], Nadine Gruteser[b], Arnd Baumann[b], Andreas Offenhäusser[a]

[a] Institute of Complex Systems ICS-8, Forschungszentrum Jülich, Leo-Brandt-Str., 52428 Jülich, Germany
[b] Institute of Complex Systems ICS-4, Forschungszentrum Jülich, Leo-Brandt-Str., 52428 Jülich, Germany

ARTICLE INFO

Article history:
Received 25 April 2016
Received in revised form 29 June 2016
Accepted 1 July 2016
Available online 11 July 2016

Keywords:
Electrophysiology
Neuronal networks
Channelrhodopsin

ABSTRACT

In recent years, optogenetic approaches have significantly advanced the experimental repertoire of cellular and functional neuroscience. Yet, precise and reliable methods for specific expression of optogenetic tools remain challenging. In this work, we studied the transduction efficiency of seven different adeno-associated virus (AAV) serotypes in primary cortical neurons and revealed recombinant (r) AAV6 to be the most efficient for constructs under control of the cytomegalovirus (CMV) promoter. To further specify expression of the transgene, we exchanged the CMV promoter for the human synapsin (hSyn) promoter. In primary cortical-glial mixed cultures transduced with hSyn promoter-containing rAAVs, expression of ChR2opt (a Channelrhodopsin-2 variant) was limited to neurons. In these neurons action potentials could be reliably elicited upon laser stimulation (473 nm). The use of rAAV serotype alone to restrict expression to neurons results in a lower transduction efficiency than the use of a broader transducing serotype with specificity conferred via a restrictive promoter. Cells transduced with the hSyn driven gene expression were able to elicit action potentials with more spatially and temporally accurate illumination than neurons electrofected with the CMV driven construct. The hSyn promoter is particularly suited to use in AAVs due to its small size. These results demonstrate that rAAVs are versatile tools to mediate specific and efficient transduction as well as functional and stable expression of transgenes in primary cortical neurons.

1. Introduction

Optogenetic approaches have promoted *in vitro* and *in vivo* experiments investigating cellular signaling and neuronal network activity with high temporal and spatial resolution (Arenkiel et al., 2007; Gradinaru et al., 2007; Madisen et al., 2012; Avermann et al., 2012; Huber et al., 2008; Desai et al., 2011; Lin et al., 2013; Dawydow et al., 2014; Renault et al., 2015). Beyond modulating and monitoring neuronal network properties, optogenetic methods have been applied to control signaling in sperm (Jansen et al., 2015) and to stimulate gene expression (Folcher et al., 2014; Konermann et al., 2013; Ye et al., 2011). Optogenetic experiments, however, require efficient introduction and expression of light-sensitive proteins into cells or tissue.

The blue light-gated cation channel Channelrhodopsin-2 (ChR2) is an intensely studied optogenetic tool (Nagel et al., 2003, 2005b; Boyden et al., 2005; Li et al., 2005; Petreanu et al., 2007; Ishizuka et al., 2006; Dawydow et al., 2014). The heterologous expression of ChR2 in electrogenic cells such as neurons can be utilized to depolarize the cell's membrane potential, thereby evoking action potentials (Zhang et al., 2006; Wang et al., 2007). Since its discovery, numerous ChR2 variants have been engineered to improve properties, such as expression level, closing dynamics (Dawydow et al., 2014; Gunaydin et al., 2010), and stable photo-switching (Berndt et al., 2009). In addition to triggering action potentials, ChR2 can be employed to silence neuronal activity by changing its ion selectivity to anions (Wietek et al., 2014; Berndt et al., 2014). Fluorescent tags such as mKate and YFP fused to ChR2 have been used to identify cells expressing ChR2 and to assess its subcellular distribution

* Corresponding author.
E-mail addresses: lei.jin@fz-juelich.de (L. Jin), wienke.lange@web.de (W. Lange), Annika.meisenberg@gmail.com (A. Kempmann), v.maybeck@fz-juelich.de (V. Maybeck), guenther_a@gmx.net (A. Günther), nadine.gruteser@t-online.de (N. Gruteser), a.baumann@fz-juelich.de (A. Baumann), a.offenhaeusser@fz-juelich.de (A. Offenhäusser).

http://dx.doi.org/10.1016/j.jbiotec.2016.07.001

(Shcherbo et al., 2007; Nagel et al., 2005a), as light-induced manipulation of neuronal electrical activity depends on the expression level of ChR2 in the cell membrane (Lin et al., 2013).

Furthermore, powerful gene delivery approaches are required for effective optical control of neuronal activity. However, standard transfection strategies can be problematic due to low cell viability and low specificity, especially for primary post-mitotic neurons (Watanabe et al., 1999; Martinez and Hollenbeck 2003; Hamm et al., 2002; Zeitelhofer et al., 2009; Karra and Dahm 2010). Therefore, we assessed recombinant adeno-associated viruses (rAAVs) as a tool for gene transfer. AAVs are non-pathogenic, have a low immunogenicity, and are known to transduce dividing and non-dividing cells (Blacklow et al., 1968; During 1997; Hernandez et al., 1999). There are numerous serotypes with different tissue tropisms, permitting specific transduction of a wide range of cell types (Howard et al., 2008); reviewed in Asokan et al. (2012).

In this work, we identified rAAV6 as the most efficient serotype for transduction of cortical-glial mixed cultures. We were first concerned which serotype of rAAV was most efficient at transducing cortical neurons. Therefore, we used the constitutively active cytomegalovirus (CMV) promoter (Wilkinson and Akrigg, 1992) to drive ChR2opt gene expression. The protein was detected to varying degrees in neurons as well as in glia cells from each of the applied serotypes. After exchanging the CMV promoter for the human synapsin (hSyn) promoter, ChR2opt expression was restricted to neurons, without loss of transduction efficiency. Other restrictive promoters might be considered as well, *e.g.* FNPY or CamKIIa, but the compact size of hSyn (only 485 bp, *vs.* approx. 2600 bp for FNPY (Nathanson et al., 2009) and 1290 bp for CamKIIa (Yizhar et al., 2011)) is favorable for packaging, even large gene constructs into AAV virions. Here, we succeeded in controlling electrical activity in primary cortical neurons expressing ChR2opt and in triggering action potentials by blue light stimulation of ChR2opt. Using this strategy, we were able to trigger responses at the single cell level with high temporal accuracy.

2. Materials and methods

2.1. Cortical cultures

Primary cortical cultures were prepared as described previously (Brewer et al., 1993). Briefly, cortices from embryonic day 18 (E18) Wistar rat (Charles River, Germany) brains were dissected and mechanically dissociated by trituration with a fire-polished, silanized pasteur pipette in 1 ml Hank's balanced salt solution without calcium or magnesium (HBSS-) (0.035% sodium bicarbonate, 1 mM pyruvate, 10 mM HEPES, 20 mM glucose, pH 7.4). The cell suspension was diluted 1:2 in HBSS+ (with calcium and magnesium) and non-dispersed tissue was allowed to settle for 3 min. The supernatant was centrifuged for 2 min at 200*g*. The pellet was resuspended in 1 ml Neurobasal medium (Gibco, Paisley, UK) with 1% B-27 (Gibco, Grand Island, NY, USA) and 0.5 mM L-glutamine (Gibco, Paisley, UK) and 50 μg/ml gentamicin (Sigma, Steinheim, Germany) (NB) per hemisphere. The cells were counted in a Neubauer counting chamber and plated in a concentration of 50,000 cells per well (24-well-plate) on poly-D-lysine (PDL, 10 μg/ml) coated 12 mm coverslips. Cells were kept at 37 °C, 5% CO_2 and 100% humidity in 500 μl NB. After 4 h, the medium was exchanged for 500 μl NB/well. Every third day, half of the medium was exchanged or, for rAAV transduced cultures, 100 μl NB medium was added in order to keep the neurons maximally exposed to the initially added rAAV particles.

This work was carried out with the approval of the Landesumweltamt für Natur, Umwelt und Verbraucherschutz Nordrhein-Westfalen, Recklinghausen, Germany, in accordance with §6 TierschG., §4 TSchG i.V. and §2 TierSchVerV.

2.2. Plasmids and cloning

Codon optimization for expression in mammalian cells was performed on the H134R variant of Channelrhodopsin-2 from *C. reinhardtii* using the software package JCat (Grote et al., 2005). In order to facilitate identification of transfected cells without significant spectral overlap with Channelrhodopsin-2 absorbtion, the fluorescent protein mKATE was fused to the C-terminus of the channel. A linker of 15 nucleotides encoding the amino acid residues AVATI was inserted to separate the channel from the fluorophore mKATE. The 3′ end of mKATE was extended by 21 nucleotides coding for a FCYENEV motif that has been shown to serve as an ER export signal in a vertebrate potassium channel (Gradinaru et al., 2010). The final construct, which we deem ChR2opt, was synthesized by GeneArt AG (Regensburg, Germany) and subcloned into the TRex system's TetON plasmid backbone (Invitrogen, Darmstadt, Germany). This construct was validated in electrofection experiments using Lonza's Rat Nucleofector Kit and patch clamp electrophysiology in both HEK293 cells and primary cortical neurons. The gene encoding portion of the construct was then further subcloned to allow for packaging into AAV vectors.

The rAAV vector pscAGFPFG2 was kindly provided by Dr. Hildegard Büning (Labor für AAV-Vektorentwicklung, CMMC, Cologne, Germany). The pAAV-hSyn-RFP construct was obtained from Addgene (Addgene plasmid #22907). ChR2opt is available in Addgene plasmid #67958. The rAAV vectors psc-CMV-ChR2opt and psc-hSyn-ChR2opt were generated using restriction digest-based strategies. For the generation of the psc-CMV-ChR2opt vector, the ChR2opt-encoding fragment was inserted into the pscAGFPFG2 vector after excision of GFP. Based on this plasmid, the psc-hSyn-ChR2opt vector was generated by exchanging the CMV promoter for the hSyn promoter fragment.

2.3. Viral vector generation

Recombinant adeno associated viral (rAAV) vectors were generated by transient transfection of HEK293 cells (obtained from ATCC). HEK293 cells were cultivated in DH10 medium (DMEM + Glutamax (Invitrogen), 10% (v/v) FBS (Gibco), 1% (v/v) antibiotics/antimycotics (Invitrogen)) at 37 °C, 5% CO_2, and 95% relative humidity. Briefly, 24 h prior to transfection 10^7 cells were seeded on Ø 14.5 cm dishes (10 dishes/rAAV construct). Cells were triple-transfected with the vector plasmid providing the transgenic viral genome, as well as the helper plasmids pRC (Girod et al., 1999) and pXX6-80 (Xiao et al., 1998), using the calcium phosphate method modified from (Chen and Okayama, 1987). Plasmid DNA was diluted in $CaCl_2$ (250 mM) and HEPES-buffered saline (50 mM HEPES, 280 mM NaCl, 1.5 mM Na_2HPO_4, pH 7.12), incubated for 3 min at RT, and added to HEK293 cells. After 24 h incubation at 37 °C, 5% CO_2, and 95% relative humidity, the medium was exchanged for DH10 with reduced FBS (DMEM + Glutamax, 2% (v/v) FBS, 1% (v/v) antibiotics/antimycotics). Cells were harvested in PBS-M/K (in mM: NaCl 130, KCl 2.5, $MgCl_2$ 1, Na_2HPO_4 70, NaH_2PO_4 30, pH 7.4) after 24 h and collected by centrifugation.

Cells were lyzed in lysis buffer (in mM: NaCl 150, Tris/HCl 50, pH 8.5) by four freeze/thaw-cycles in liquid nitrogen and at 37 °C. Nucleic acids were digested with benzonase (50 U/ml; Merck) for 30 min at 37 °C. After removal of cell debris by centrifugation rAAV particles were enriched by density gradient centrifugation. The rAAV suspension was sub-layered with iodixanol (Sigma-Aldrich, Taufkirchen, Germany) solutions (15%, 25%, 40%, and 60% iodixanol) and centrifuged (264,000*g*, 4 °C, 2 h). The 40% iodixanol phase containing the virus particles

was collected and viral titers were determined by quantitative PCR. Briefly, viral genomes were isolated using the DNeasy Blood & Tissue Kit (Qiagen, Hilden, Germany) and genomic titers were determined. Primer pairs framing defined DNA segments of promoter or transgene sequences were used: for the CMV promoter (CGCTATTACCATGGTGATGCG, CCTCCCACCGTACACGCC), for the hSyn promoter (CCTGCGTATGAGTGCAAGTG, GGTGCTGAAGCTGGCAGTG), and for the eGFP-encoding sequence (GACGTAAACGGCCACAAGTTC, GAAGTCGTGCTGCTTCATGTG).

2.4. AAV transduction

Primary cortical cells, grown on PDL coated coverslips (12 mm), were transduced with rAAVs on DIV1 or DIV8 with different multiplicities of infection (MOI). The medium (500 μl) was completely exchanged with NB containing 10^7, 10^8, 10^9, 10^{10} or 10^{11} viral genomes to achieve MOIs of 2×10^2, 2×10^3, 2×10^4, 2×10^5 and 2×10^6 viral particles per cell (vp/cell), respectively. As a control, the same volume of 40% iodixanol was added to individual wells. Three days post transduction (DPT), 100 μl NB medium was added. The cells were electrophysiologically measured after DIV14 or fixed for immunofluorescence DPT7-9.

2.5. Electrophysiology

Whole cell patch clamp experiments were performed using an EPC9 amplifier (HEKA Elektronik, Lambrecht/Pfalz, Germany) controlled by the TIDA 5.240 software (HEKA Elektronik) (Zhu et al., 2016). Cortical neurons were recorded between DIV14 and 16 in the current clamp mode (with a holding membrane current leading to a membrane potential of −70 mV). The recordings were performed in extracellular patch clamp buffer solution (mM: NaCl 120, KCl 3, $MgCl_2$ 1, HEPES 10, $CaCl_2$ 2; pH 7.3, 248 mosm kg^{-1}). Patch pipettes were pulled from borosilicate glass capillaries (Sutter Instrument Co., Novato, CA, USA) using a micropipette puller (P-2000, Sutter) to achieve a pipette resistance of 6–9 MOhm. The pipettes were filled with intracellular patch solution (mM: NaCl 2, KCl 120, $MgCl_2$ 4, HEPES 5, EGTA 0.2, Mg-ATP 0.20, pH 7.3, 255 mosm kg^{-1}). Cells were excluded if the membrane resistance was outside of the range from 50 MOhm to 300 MOhm and the series resistance of neurons was higher than 26.4 MOhm. Spiking was measured while injecting current to keep the voltage of neurons at approximately −70 mV (holding current ranging from 0 pA to −200 pA).

2.6. Laser stimulation

ChR2opt-expressing neurons were randomly chosen and stimulated with a 473 nm diode laser (Rapp OptoElectronic GmbH, Hamburg, Germany) which was guided through an optical fiber and reflected with a dichroic mirror (UGA-40, Rapp OptoElectronic GmbH) into the light path of a Zeiss Axioscope microscope equipped with an Olympus (x20) objective (UMPLFLN20xW). The laser spot diameter was adjusted to about 24 μm, resulting in a laser intensity of approximately 1.74 W mm^{-2}. Different delay times (150 ms or 200 ms or 500 ms) and different laser pulse times (ranging from 1 ms to 50 ms) were applied for ChR2opt stimulation targeting somas/axons/dendrites.

2.7. Immunofluorescence

For the immunostaining, cells were fixed with 4% (w/v) paraformaldehyde in PBS (PFA) at RT for 20 min, washed with 1 x PBS (pH 7.4) and blocked overnight in blocking solution (1% (w/v) BSA, 2% (v/v) goat serum in PBS). Cells were permeabilized with 0.1% (w/v) TritonX-100 in blocking buffer for 15 min. The following primary antibodies were used: rabbit anti-MAP2 (Catalogue number: AB5622, dilution 1:500, Chemicon/Millipore) and mouse anti-GFAP (Catalogue number: MAB3402, dilution 1:100, Chemicon/Millipore). Bound primary antibodies were visualized using Alexa-488 (A-11029), Alexa-546 (A-11003) or Alexa-633 (A-21071)-conjugated secondary antibodies (Life technologies, Eugene, Oregon, USA; dilution 1:500 in blocking solution). Nuclei were stained with TOPRO (Life technologies, Eugene, Oregon, USA; dilution 1:500 in blocking solution). Samples were mounted in Dako Fluorescence Mounting Medium (Agilent Technologies, Waldbronn, Germany) and analyzed by using a Zeiss Apotome microscope (Carl Zeiss Microscopy GmbH, Göttingen, Germany) or Confocal laser scanning microscope (Leica TCS SP5, Leica Microsystems, Heidelberg, Germany).

3. Results

3.1. Transduction efficiency of rAAV serotypes in primary cortical cultures

We were able to show proof of principle stimulation of neurons expressing ChR2opt after electrofection with ChR2opt encoding plasmid constructs. However, the area of membrane necessary for illumination and the duration of illumination were not satisfactory for high precision stimulation. Therefore, we sought alternatives to improve expression levels that eventually could reduce the area and duration of illumination necessary to trigger a light-evoked action potential. In order to achieve this goal, we wanted to evaluate the transduction efficiencies of different rAAV serotypes in rat primary cortical cultures that contained both neurons and glia. Initially, rAAV serotypes 1, 2, 4, 5, 6, 8, and 9 mediating expression of eGFP under the control of the CMV promoter were investigated. Viral vectors were applied with different multiplicity of infection (MOI) values, *i.e.* 2×10^3, 2×10^4, 2×10^5 and 2×10^6 vp/cell, on cortical-glial mixed cultures after 8 days *in vitro* (DIV8). All of the applied rAAV serotypes mediated expression of eGFP, but transduction efficiencies and eGFP expression levels varied between serotypes (Table 1 and Fig. S1). Due to the constitutively active CMV promoter eGFP expression was observed in neuronal, as well as glial cells. The ratio of transduced neuronal *vs.* transduced glial cells was examined using a neuronal marker (microtubule-associated protein 2, MAP2) and an astrocyte marker (glial fibrillary acidic protein, GFAP). Serotype 6 mediated the most efficient transduction in primary cortical-glial mixed cultures (Table 1 and Fig. 1). However, even though the highest neuron transduction rate was observed for serotype 6, glial cells were also transduced (Fig. 1). Therefore, the serotype-dependent tropism was a first step towards a cell-type (here neuron) specific transgene expression.

3.2. Neuron-specific expression of ChR2opt in primary cortical neurons

Based on the results described above, we selected rAAV6 for transgene expression in cortical neurons. For optogenetic approaches, we generated a rAAV6 vector to express ChR2opt under the control of the CMV promoter. The rAAV6-CMV-ChR2opt construct mediated expression of the transgene in about 83% of neurons. Immunocytochemical staining revealed that ChR2opt was mainly expressed in neuronal cells, but also in about 63% of GFAP-positive cells (Fig. 2 and Fig. 3B). Fluorescence of the C-terminal mKate tag could be detected on DPT3 and increased until DPT7. These results corroborate the data for CMV promoter-mediated eGFP expression after transduction with different rAAV serotypes (Table 1 and Fig. S1).

Table 1
Transduction efficiency of different rAAV serotypes in primary cortical-glial mixed cultures.

Serotype	Expression level	Transduced neurons (total MAP2 positive)	Transduced glial cells (total GFAP positive)
1	++	++	+++
2	+	+	++
4	+	+	+++
5	+	+	+
6	+++	+++	++
8	+	+	–
9	+	+	+++

Primary cortical-glial mixed cultures were transduced on DIV8 with rAAV serotypes 1, 2, 4, 5, 6, 8, and 9 expressing eGFP under the control of the CMV promoter (MOI 2×10^4 vp/cell). Transduction efficiencies were estimated based on eGFP fluorescence (DPT9). Cell types were identified using the neuronal marker MAP2 and the glial marker GFAP. Percentages of transduced neurons and glial cells were estimated based on total MAP2 or GFAP-positive cells, respectively. Mean values ($n = 3$ independent experiments; each one includes three samples) were calculated and are depicted as – (no transduced cells), + (≤ 30%), ++ (30–66%), and +++ (≥ 66%).

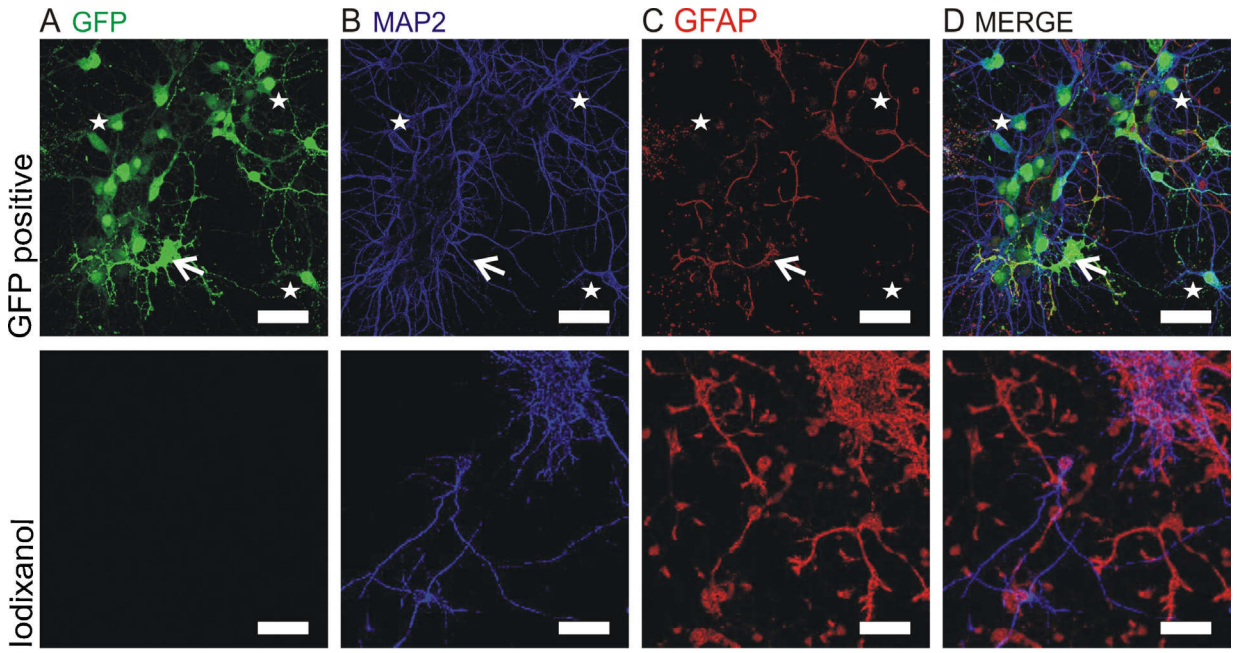

Fig. 1. Expression of eGFP in primary cortical-glial mixed cultures.
Primary cortical-glial mixed cultures were transduced with rAAV6-CMV-eGFP (MOI 2×10^4 vp/cell) on DIV8 (upper panel) or treated with iodixanol as a control (lower panel). Immunocytochemistry was performed on DIV15 and cultures were stained using specific antibodies for MAP2 (B, blue) and GFAP (C, red). Fluorescence of eGFP is shown in green (A) and the merged images are depicted in (D). Arrows identify eGFP-positive glial cells and asterisks mark eGFP-expressing neurons. Scale bars indicate 50 μm. (For interpretation of the references to colour in this figure legend, the reader is referred to the web version of this article.)

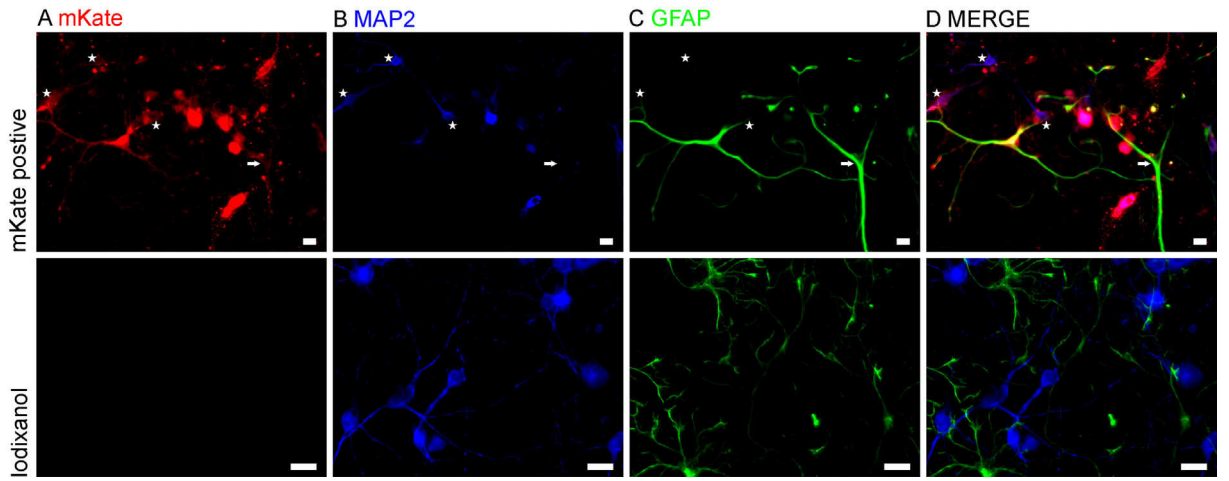

Fig. 2. Expression of ChR2opt in primary cortical-glial mixed cultures.
Primary cortical-glial mixed cultures were transduced with rAAV6-CMV-ChR2opt (MOI 2×10^4 vp/cell) on DIV8 (upper panel) or treated with iodixanol as a control (lower panel). Immunocytochemistry was performed on DIV15 and cultures were stained using specific antibodies for MAP2 (B, blue) and GFAP (C, green). Fluorescence of mKate is shown in red (A) and the merged images are depicted in (D). Arrows identify mKate-positive glial cells and asterisks mark mKate-expressing neurons. Scale bars indicate 20 μm. For typical staining of cells without rAAV and without iodixanol treatment, see Fig. S2. (For interpretation of the references to colour in this figure legend, the reader is referred to the web version of this article.)

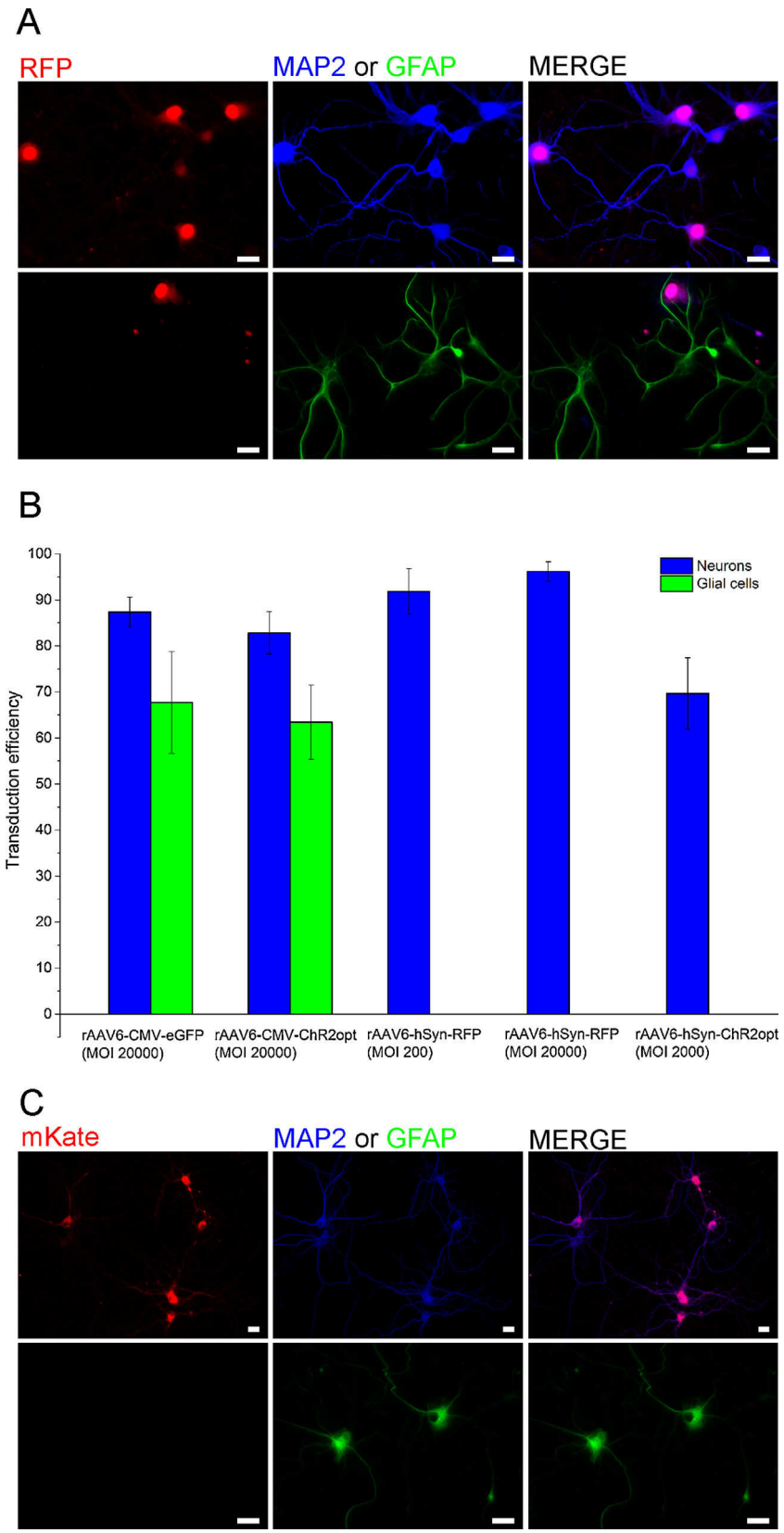

Fig. 3. Neuron-specific expression of ChR2opt in primary cortical-glial mixed cultures.
(A) Primary cortical-glial mixed cultures were transduced with rAAV6-hSyn-RFP (MOI 2×10^4 vp/cell) on DIV8 and stained immunocytochemically on DIV14 for MAP2 (blue, top, middle) and GFAP (green, bottom, middle). Fluorescence of RFP is shown in red and the merged images are depicted on the right. Scale bars indicate 20 μm. (B) Neuron transduction efficiencies of rAAV6 vectors (DIV14) harboring different promoters. The data are mean values ± SEM ($n = 3$ independent experiments. In one experiment, 10 different areas of each coverslip containing neurons were imaged for analysis). (C) Primary cortical-glial mixed cultures were transduced with rAAV6-hSyn-ChR2opt (MOI 2×10^3 vp/cell) on DIV8 and stained immunocytochemically on DIV15. Autofluorescence of mKate is depicted in red, MAP2 staining in blue (top, middle), and GFAP staining in green (bottom, middle). The merged images are shown on the right. Scale bars indicate 20 μm. (For interpretation of the references to colour in this figure legend, the reader is referred to the web version of this article.)

Subsequently, we substituted the CMV promoter for the neuron-specific human synapsin 1 (hSyn) promoter to further improve neuronal expression levels while reducing glial ChR2opt expression. Firstly, we assessed the expression pattern of a rAAV6-hSyn-RFP construct in primary cortical-glial mixed cultures based on RFP fluorescence. Immunocytochemical staining with MAP2 and GFAP antibodies revealed a very high percentage of RFP-positive neurons, whereas glia cells did not express the fluorescent protein (Fig. 3A). The neuron transduction efficiency of 92% ± 5% achieved with rAAV6-hSyn-RFP (MOI 2×10^2 vp/cell) was higher than observed for rAAV6-CMV-eGFP (MOI 2×10^4 vp/cell). Application of rAAV6-hSyn-RFP with an MOI of 2×10^4 vp/cell further increased the neuron transduction efficiency to 96% ± 2% (Fig. 3B). In summary, the hSyn promoter not only mediated neuron-specific transgene expression but also seemed to improve transduction and/or expression efficiency compared to the CMV construct. Next, we probed whether ChR2opt could also be specifically expressed in primary rat cortical neurons with the hSyn promoter via rAAV6-mediated transduction. A transduction efficiency of 70% ± 8% was achieved (Fig. 3B). As depicted in Fig. 3C, mKate fluorescence was clearly visible in neurons while glial cells did not express the protein. This result is the same as what we observed for hSyn-RFP expression (Fig. 3A).

3.3. Optical stimulation of ChR2opt-expressing neurons

In order to test for ChR2opt functionality in triggering action potentials, we performed optical stimulation experiments. Single ChR2opt-expressing neurons were stimulated using blue laser light (473 nm) with a spot size of approximately 24 μm in diameter (laser intensity of 1.74 W mm^{-2}). Cells were analyzed using the whole cell patch clamp technique.

We probed how many action potentials (= spikes) were elicited with different light pulse durations using the same interstimulus delay times for ChR2opt recovery. In Fig. 4A experiments are shown where ChR2opt was expressed under the control of the CMV promoter (rAAV6-CMV-ChR2opt). Two different delay times (150 ms or 200 ms) and five different laser pulse times (ranging from 1 ms to 30 ms) were applied for ChR2opt stimulation. Spikes were more easily evoked with longer pulse times than with shorter pulse times. Using a 10 ms laser pulse, spikes were triggered with a success rate of 83% ± 8%. Successive stimuli were applied with interpulse delay times of 150 ms. The stimulation success rate increased to 97% ± 2% if the delay time was extended to 200 ms. Accordingly, measurements of cells transduced with rAAV6-hSyn-ChR2opt were performed with stimulation pulses interrupted with delay times of 200 ms. Under these conditions, pulse times of ≥5 ms resulted in successful spike generation rates of up to 99%. Furthermore, we addressed eventual triggering of extra spikes. As depicted in Fig. 4B pulse times of 50 ms evoked an extra spike. Using 30 ms pulses, a second depolarization was measured but it did not reach the threshold level to induce another action potential. The photocurrent of Channelrhodopsin consists of a peak current and a stationary current (Berndt et al., 2011). Our data suggest that during the stationary photocurrent that can be induced with a longer stimulation pulse, some channels remain open. These channels may keep the cell depolarized and trigger an additional action potential especially when long light stimuli (50 ms) are applied.

Having demonstrated the ability of ChR2opt to trigger action potentials at the soma, we next investigated whether illumination of axons or dendrites of a transduced neuron were sufficient to evoke action potentials. Five different sites including the soma of a ChR2opt expressing neuron were selected for stimulation (Fig. 5A, asterisks). Action potentials were recorded at the soma with whole cell patch clamping. As we had demonstrated before (Lange et al., 2014), action potentials could be precisely and repeatedly triggered at each of 5 different sites with 100 laser pulses of 50 ms duration and a delay time of 500 ms (Fig. 5B). We also examined the dependence of the response time and spike amplitude to the distance of the stimulation site. The time from the onset of illumination to spike peak measured at the soma was defined as response time. As depicted in Fig. 5C, response times decreased with smaller distances between the stimulation site and the patch pipette. Stimulation at position 5 (see Fig. 5A) triggered an action potential after 18.4 ± 0.2 ms, whereas stimulation at the soma (position 1) caused an action potential approximately after 12.1 ± 0.2 ms. The amplitudes of the action potentials were very similar and were independent of the stimulation site (Fig. 5D). Similar effects were

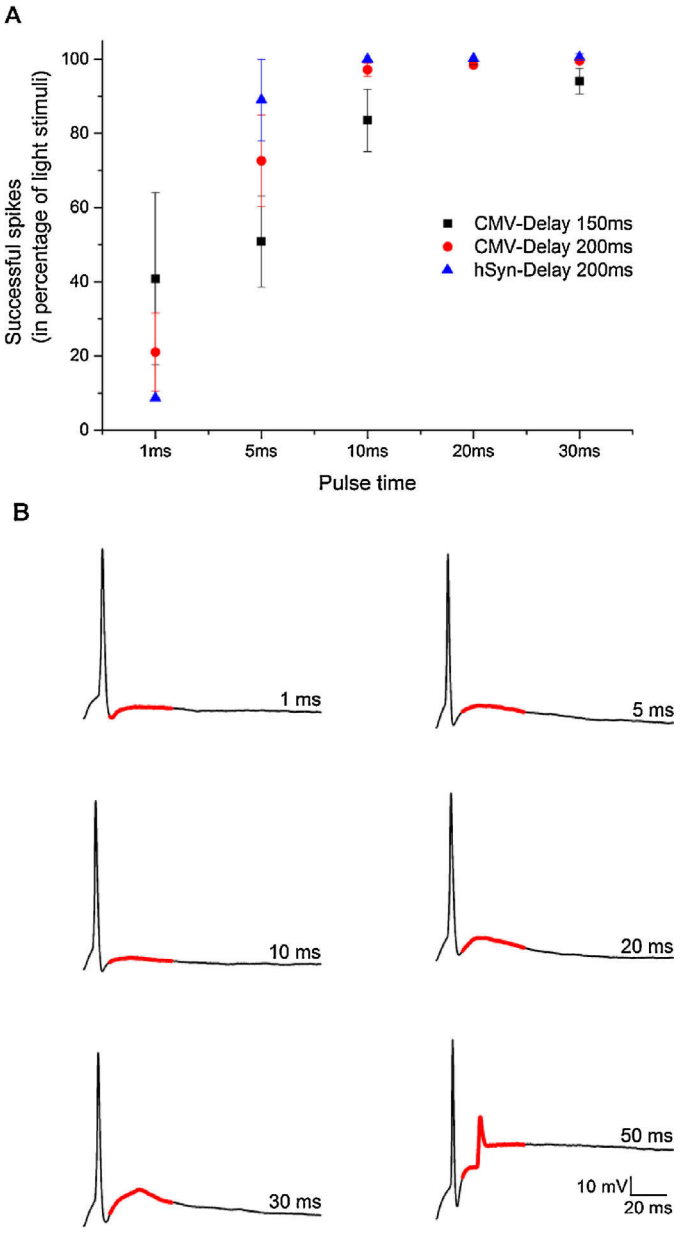

Fig. 4. Stimulation of ChR2opt – expressing neurons.
(A) Neurons transduced with a rAAV6 construct harboring either the CMV promoter (black, red) or the hSyn promoter (blue) were examined. Successful generation of action potentials (%) is displayed *vs.* pulse duration of the light stimulus. Data (n = 3–7 cells for rAAV6-CMV-ChR2opt group; n = 3–4 cells for rAAV6-hSyn-ChR2opt group) are presented as mean ± SEM. Each stimulation was repeated 100 times. (B) An extra spike was triggered by longer pulse times in a rAAV6-CMV-ChR2opt transduced neuron. (For interpretation of the references to colour in this figure legend, the reader is referred to the web version of this article.)

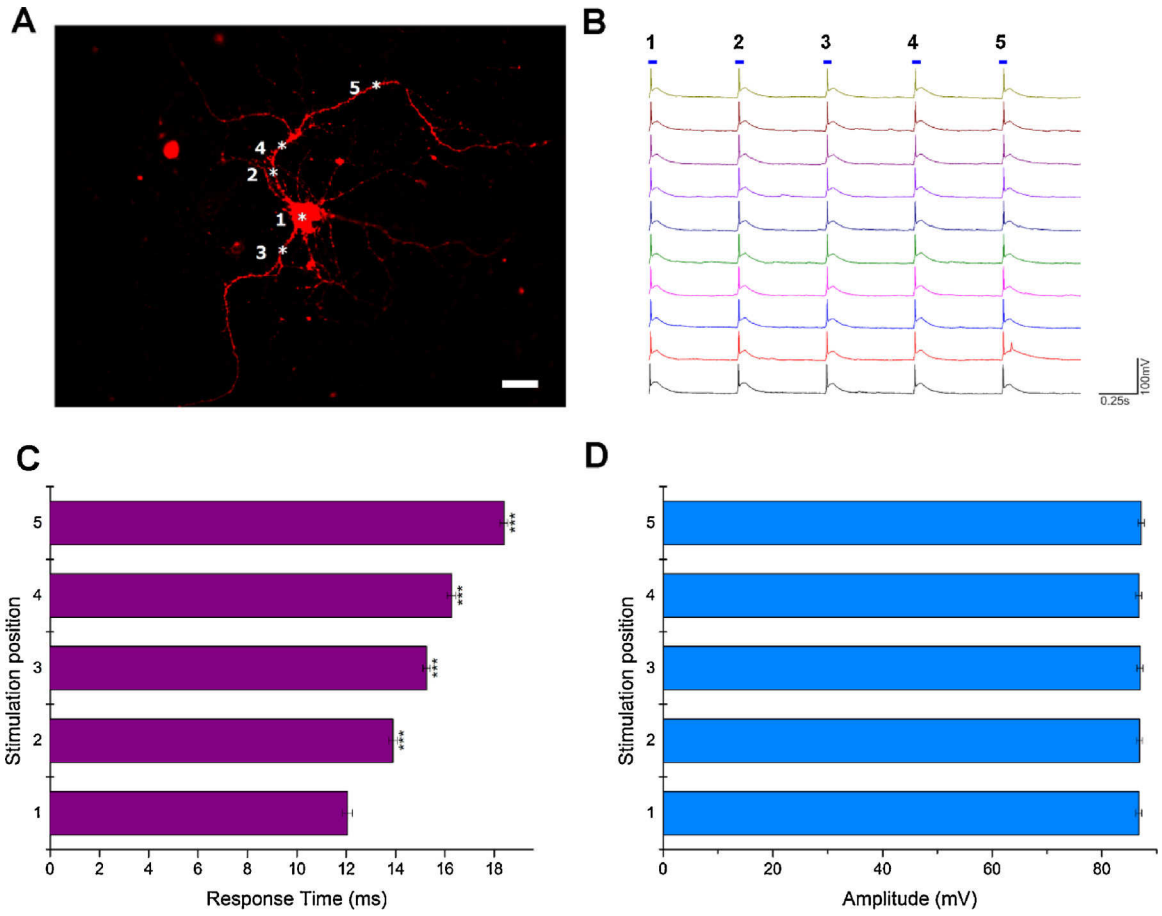

Fig. 5. Stimulation of rAAV6-CMV-ChR2opt-transduced neurons.
(A) Autofluorescence of mKate tagged to ChR2opt is displayed. The five stimulation sites are indicated by asterisks (positions 1–5). The scale bar represents 50 μm. (B) Voltage traces of 10 successive stimulations (50 ms pulses with 500 ms interpulse delay times) initiated at the 5 different stimulation sites (see Fig. 5A) were recorded from a single cell by whole cell patch clamping. (C) Response time to evoke an action potential measured at the soma after light stimulation (473 nm) at each of the five different stimulation sites (see Fig. 5A) (one-way ANOVA, $p < 0.001$) are depicted. (D) Action potential amplitudes measured after light stimulation (473 nm) at each of the 5 different stimulation sites are shown. Data ($n = 50$ trials from one cell) are presented as mean ± SEM. (For interpretation of the references to colour in this figure legend, the reader is referred to the web version of this article.)

seen on additional cells tested independently with varying numbers of illumination points distant from the soma ($n = 4$). However, since each response is dependent on cell morphology and the exact position illuminated during stimulation, it is not possible to pool distance vs. delay data across cells.

Similar to CMV-driven expression of ChR2opt, neurons transduced with rAAV6-hSyn-ChR2opt generated action potentials after stimulation with blue laser light ($n = 15$). In Fig. 6A a representative trace is depicted using a laser pulse of 50 ms and a delay time of 500 ms. When applying 50 ms pulses, again, often more than one spike was evoked. The success rate of triggering the first spike was 100%, whereas the success rate to trigger a second spike was 55% ± 22% (Fig. 6B). A comparison of the FWHM (Full-Width Half-Maximum) and the amplitude of both the first and second spike after light stimulation revealed that the FWHM of the first spike was smaller than that of the second one (Fig. 6C), while the amplitude of first spike was larger than that of the second one (Fig. 6D).

4. Discussion

Recombinant AAV vectors are promising tools for gene delivery both, *in vitro* and *in vivo*. Multiple naturally occurring serotypes have been demonstrated to target cells in different tissues and organs, including the brain (Aschauer et al., 2013; Schultz and Chamberlain 2008). The transduction efficiency of cells or tissue strongly depends on the AAV serotype and its binding partners on the cell surface (Cearley and Wolfe, 2006). In this work, we have examined the transduction efficiency of different rAAV serotypes in rat primary cortical-glial mixed cultures and found that rAAV6 is best suited to gain high-efficiency transduction rates. AAV5 has been used as a safe and effective viral vector for transgene expression in the brains of non-human primates (Diester et al., 2011). However, rAAV5 showed the lowest efficiency for transgene expression in rat primary cortical-glial mixed cultures (Table 1). Mechanical preparation of the primary cortical neurons preserves their surface proteins, therefore we do not expect a significant difference in transduction rate *in vivo* compared to our *in vitro* tests. Comparative studies using different AAV serotypes and adenoviruses as well as lentiviruses showed that AAVs were advantageous when testing transduction efficacy and stability of gene expression (Doherty et al., 2011; Ehrengruber et al., 2001; Mason et al., 2010; Vandendriessche et al., 2007). We used a similar approach as applied by (Mason et al., 2010) to examine which rAAV serotype would efficiently transduce cortical-glial mixed cultures. The rAAV6 serotype including the neuron-specific promoter hSyn turned out to be the most efficacious viroid. Applying viral suspensions to our *in vitro* cultures did not impair viability of the samples for up to 3 weeks. Since rAAVs can also be administered to living animals either by systemic or tissue-limited injection, such approaches would tremendously reduce the time required to gen-

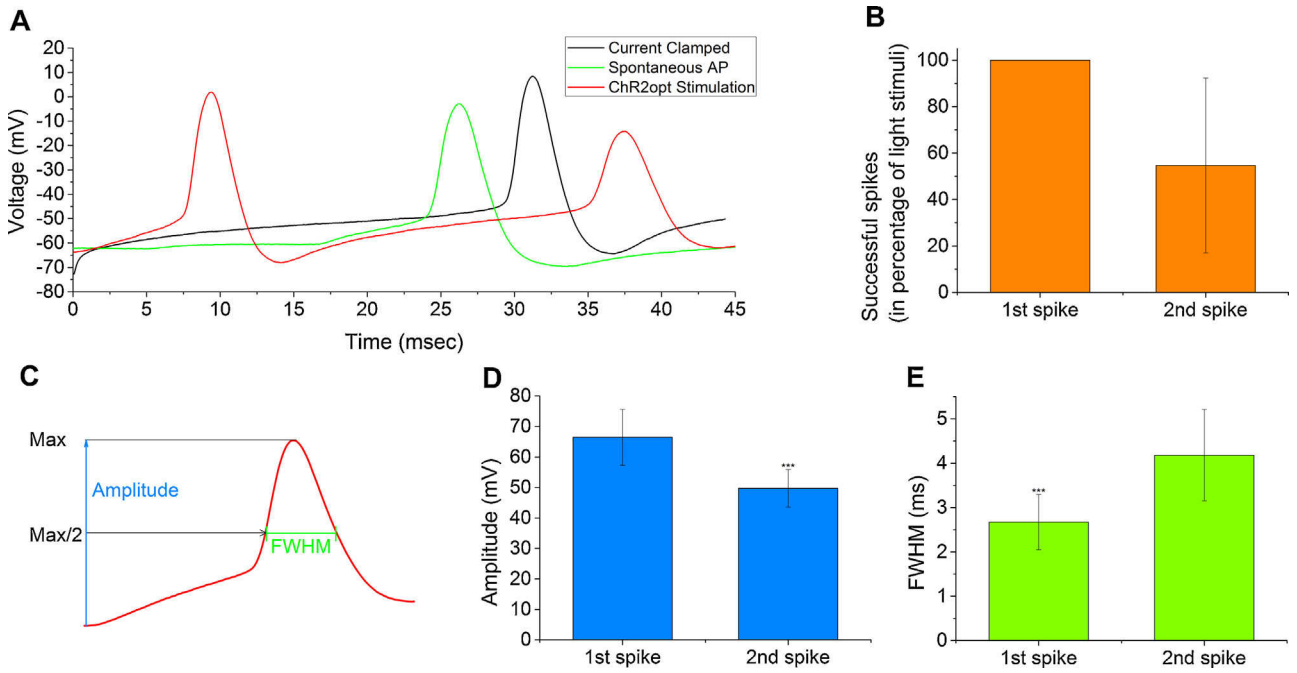

Fig. 6. Triggering action potentials in rAAV6-hSyn-ChR2opt transduced neurons.
(A) Comparison of action potentials in a typical rAAV6-hSyn-ChR2opt transduced neuron. A voltage trace (black) driven by 80 pA injection from the patch pipette, a representative voltage trace (red) of APs evoked by laser pulse application for 50 ms separated by a delay time of 500 ms, and a spontaneous action potential (green) are shown. (B) Success rate (%) of action potential generation in response to a light stimulus is depicted for the first and second spike. (C) The scheme of the amplitude and FWHM (Full-Width at Half-Maximum) in one spike are depicted in blue and green color, respectively. 'Max' indicates the maximum of depolarization from the resting potential. (D) Amplitudes of the first and second spikes (one-way ANOVA, $p < 0.001$) were analyzed. (E) FWHM of the first and second spikes (one-way ANOVA, $p < 0.001$) is shown. Data ($n = 300$ spikes from one cell for the first spike group; $n = 164$ spikes from the same cell for the second spike group) are presented as mean ± SD. (For interpretation of the references to colour in this figure legend, the reader is referred to the web version of this article.)

erate transgenic animals and/or breed genetically modified mouse strains for offspring to be analyzed.

The ability to transfer a target gene into a specific cell type is an essential aspect of biomedical research. The specific expression of ChR2opt in this work would be useful for the field of optogenetics. The human synapsin 1 promoter confers neuron-specific transgene expression (Kügler et al., 2003). Our data have shown that the incidence of ChR2opt or RFP expression was dramatically decreased in glial cells using the hSyn promoter (Fig. 3B). In contrast, the commonly used CMV promoter led to gene expression in neuronal as well as glial cells (Fig. 2). In addition, we observed more action potentials and even multiple action potentials in response to one light pulse in neurons that had been transduced with rAAV6-hSyn-ChR2opt rather than rAAV6-CMV-ChR2opt.

It has been described that the strength of depolarization and the delay time between two action potentials that result from ChR2 stimulation depend on the expression level of Channelrhodopsin (Lin et al., 2013). We found that CMV-driven ChR2opt expression is sufficient for generating action potentials by illuminating the axon with a pulse of blue light. The illuminated area of the axon is much smaller than the total laser spot area, which was about 450 μm^2. In contrast, light stimuli delivered to the cell's soma cover an area that has approximately the same size as the laser spot. Our data support the notion that neuronal activity can be evoked by blue light from almost any area of single, ChR2opt-expressing neurons.

In order to elicit sufficient photocurrent for depolarizing a neuron, the expression time of ChR2opt may play a significant role. Expression of the mKate tag fused to ChR2opt was already visible three days after transduction. However, a longer expression time clearly improved detection of the fluorescent tag. We observed convincing expression levels at 7DPT that is DIV15 (Fig. 2) and laser stimulation of neurons synthesizing ChR2opt reproducibly resulted in the generation of action potentials.

When stimulating different locations in one single neuron, response times were significantly different if targeting the axon/dendrites or the soma (Fig. 5C). We calculated the speed of action potential propagation from the stimulated site to the soma. These were in the range of 18–44 $\mu m\ ms^{-1}$.

When multiple spikes were elicited by a single light stimulation, the amplitude of the first spike was larger than that of the second one (Fig. 6D). The reduction in spike amplitude may indicate a depolarization block due to overly large photocurrents as has been shown for a ChR2 mutant, i.e., hSyn-ChR2(T159C) (Berndt et al., 2011). A similar reduction in the amplitude of the second spike was found when the cell was stimulated by direct current injection from the pipette. 60 or 80 pA injections resulted in multiple spikes, with a reduction of down to 74% of the initial spike ($n = 4$ pairs). The persistent photocurrent during the first spike may prevent recovery of voltage-gated sodium channels from inactivation (Bendahhou, 2012). This might imply that if the photocurrent of Channelrhodopsin is too large, it may result in ceasing neuronal activity. Since spikes were triggered with a delay of approximately 10 ms, the illumination time could be reduced to 10–15 ms to allow faster repolarization after the spike. Alternatively, this phenomena could be employed to achieve stimulation and inhibition of neurons with a single optogenetic construct. Slow acting Channelrhodopsin variants, such as those reported by Nagel et al. (2005a,b) and Lin et al. (2013) are suited to utilizing residual currents for a dual stimulation and inhibition system with a single light source.

We have observed successful transduction of primary cortical-glial mixed cultures with rAAV6 constructs. Though other serotypes showed a lower ability to transduce glia cells, the accompanying poor transduction efficiency of neurons calls for an appropriate ability to achieve neuronal expression, *e.g.*, by employing the hSyn promoter. The hSyn driven ChR2opt expression allowed us to reliably stimulate neural action potentials with short light pulses

(≥5 ms) and illumination areas down to 96 μm^2, which is the surface area of an axon or dendrite in the laser spot.

5. Conclusion

We established high-efficiency transduction and neuron-specific expression of ChR2opt mediated by the rAAV6 serotype and the hSyn promoter. Using this strategy, successful manipulation of neuronal activity with single cell selectivity and good temporal accuracy after blue light activation of ChR2opt was achieved. We demonstrated rAAV6 as a suitable vector for transferring a gene into primary cortical neurons *in vitro*. To improve the efficiency and specificity of expression, we invoked the hSyn promoter to restrict gene expression to neurons. Notably, we could more effectively control neuronal activity with the hSyn-driven than the CMV-driven ChR2opt expression. Also, additional action potentials were generated when stimulating ChR2opt transduced neurons with longer pulses of blue laser light. In conclusion, rAAV6 with hSyn promoter driven constructs provides a useful tool for specifically manipulating neuronal activity.

Competing interests

All authors declare no competing or financial interests.

Author contributions

L.J. performed all experiments on ChR2opt and most of the data analyses, and wrote the manuscript. W.L. and A.K. performed screening experiments of rAAV serotypes. A.K., A.G. and N.G. performed rAAV production. V.M. and A.B. provided significant intellectual input in the development of this study and edited the manuscript. A.O. directly supervised the study.

Funding

This work was supported by the Deutsche Forschungsgemeinschaft [grant 1541/7-3 to A.B.] and the Helmholtz Initiative on Synthetic Biology.

Acknowledgements

We kindly thank B. Breuer for the preparation of rat primary cortical neurons, L. Chen and P. Rinklin for helpful programing with MATLAB and Dr. Hildegard Büning (Labor für AAV-Vektorentwicklung, CMMC, Cologne, Germany) for support in establishing AAV production and purification.

Appendix A. Supplementary data

Supplementary data associated with this article can be found, in the online version, at http://dx.doi.org/10.1016/j.jbiotec.2016.07.001.

References

Arenkiel, B.R., Peca, J., Davison, I.G., Feliciano, C., Deisseroth, K., Augustine, G.J., Ehlers, M.D., Feng, G., 2007. In vivo light-induced activation of neural circuitry in transgenic mice expressing channelrhodopsin-2. Neuron 54, 205–218.

Aschauer, D.F., Kreuz, S., Rumpel, S., 2013. Analysis of transduction efficiency, tropism and axonal transport of AAV serotypes 1, 2, 5, 6, 8 and 9 in the mouse brain. PLoS One 8, e76310.

Asokan, A., Schaffer, D.V., Samulski, R. Jude, 2012. The AAV vector toolkit: poised at the clinical crossroads. Mol. Ther. 20, 699–708.

Avermann, M., Tomm, C., Mateo, C., Gerstner, W., Petersen, C.C.H., 2012. Microcircuits of excitatory and inhibitory neurons in layer 2/3 of mouse barrel cortex. J. Neurophysiol. 107, 3116–3134.

Bendahhou, S., 2012. Keeping hyperactive voltage-gated sodium channels in silent mode. J. Physiol. 590, 2543–2544.

Berndt, A., Yizhar, O., Gunaydin, L., a Hegemann, P., Deisseroth, K., 2009. Bi-stable neural state switches. Nat. Neurosci. 12, 229–234.

Berndt, A., Schoenenberger, P., Mattis, J., Tye, K.M., Deisseroth, K., Hegemann, P., Oertner, T.G., 2011. High-efficiency channelrhodopsins for fast neuronal stimulation at low light levels. Proc. Natl. Acad. Sci. U. S. A. 108, 7595–7600.

Berndt, A., Lee, S.Y., Ramakrishnan, C., Deisseroth, K., 2014. Structure-guided transformation of channelrhodopsin into a light-activated chloride channel. Science 344, 420–424.

Blacklow, N.R., Hoggan, M.D., Kapikian, A.Z., Austin, J.B., Rowe, W.P., 1968. Epidemiology of adenovirus-associated virus infection in a nursery population. Am. J. Epidemiol. 88, 368–378.

Boyden, E.S., Zhang, F., Bamberg, E., Nagel, G., Deisseroth, K., 2005. Millisecond-timescale, genetically targeted optical control of neural activity. Nat. Neurosci. 8, 1263–1268.

Brewer, G.J., Torricelli, J.R., Evege, E.K., Price, P.J., 1993. Optimized survival of hippocampal neurons in B27-supplemented Neurobasal™, a new serum-free medium combination. J. Neurosci. Res. 35, 567–576.

Cearley, C.N., Wolfe, J.H., 2006. Transduction characteristics of adeno-associated virus vectors expressing cap serotypes 7, 8, 9, and Rh10 in the mouse brain. Mol. Ther. 13, 528–537.

Chen, C., Okayama, H., 1987. High-efficiency transformation of mammalian cells by plasmid DNA. Mol. Cell Biol. 7, 2745–2752.

Dawydow, A., Gueta, R., Ljaschenko, D., Ullrich, S., Hermann, M., Ehmann, N., Gao, S., Fiala, A., Langenhan, T., Nagel, G., Kittel, R.J., 2014. Channelrhodopsin-2-XXL, a powerful optogenetic tool for low-light applications. Proc. Natl. Acad. Sci. U. S. A., 2–7.

Desai, M., Kahn, I., Knoblich, U., Bernstein, J., Atallah, H., Yang, A., Kopell, N., Buckner, R.L., Graybiel, A.M., Moore, C.I., Boyden, E.S., 2011. Mapping brain networks in awake mice using combined optical neural control and fMRI. J. Neurophysiol. 105, 1393–1405.

Diester, I., Kaufman, M.T., Mogri, M., Pashaie, R., Goo, W., Yizhar, O., Ramakrishnan, C., Deisseroth, K., Shenoy, K.V., 2011. An optogenetic toolbox designed for primates. Nat. Neurosci. 14, 387–397.

Doherty, F.C., Schaack, J.B., Sladek, C.D., 2011. Comparison of the efficacy of four viral vectors for transducing hypothalamic magnocellular neurosecretory neurons in the rat supraoptic nucleus. J. Neurosci. Methods 197, 238–248.

During, M., 1997. Adeno-associated virus as a gene delivery system. Adv. Drug Deliv. Rev. 27, 83–94.

Ehrengruber, M.U., Hennou, S., Büeler, H., Naim, H.Y., Déglon, N., Lundstrom, K., 2001. Gene transfer into neurons from hippocampal slices comparison of recombinant semliki forest virus, adenovirus, adeno-associated virus, lentivirus, and measles virus. Mol. Cell. Neurosci. 17, 855–871.

Folcher, M., Oesterle, S., Zwicky, K., Thekkottil, T., Heymoz, J., Hohmann, M., Christen, M., Daoud El-Baba, M., Buchmann, P., Fussenegger, M., 2014. Mind-controlled transgene expression by a wireless-powered optogenetic designer cell implant. Nat. Commun. 5, 5392.

Girod, A., Ried, M., Wobus, C., Lahm, H., Leike, K., Kleinschmidt, J., Deléage, G., Hallek, M., 1999. Genetic capsid modifications allow efficient re-targeting of adeno-associated virus type 2. Nat. Med. 5, 1438.

Gradinaru, V., Thompson, K.R., Zhang, F., Mogri, M., Kay, K., Schneider, M.B., Deisseroth, K., 2007. Targeting and readout strategies for fast optical neural control in vitro and in vivo. J. Neurosci. 27, 14231–14238.

Gradinaru, V., Zhang, F., Ramakrishnan, C., Mattis, J., Prakash, R., Diester, I., Goshen, I., Thompson, K.R., Deisseroth, K., 2010. Molecular and cellular approaches for diversifying and extending optogenetics. Cell 141, 154–165.

Grote, A., Hiller, K., Scheer, M., Münch, R., Nörtemann, B., Hempel, D.C., Jahn, D., 2005. JCat: a novel tool to adapt codon usage of a target gene to its potential expression host. Nucleic Acids Res. 33, W526–W531.

Gunaydin, L.A., Yizhar, O., Berndt, A., Sohal, V.S., Deisseroth, K., Hegemann, P., 2010. Ultrafast optogenetic control. Nat. Neurosci. 13, 387–392.

Hamm, A., Krott, N., Breibach, I., Blindt, R., Bosserhoff, A.K., 2002. Efficient transfection method for primary cells. Tissue Eng. 8, 235–245.

Hernandez, Y.J., Wang, J., Kearns, W.G., Loiler, S., Poirier, A., Flotte, T.R., 1999. Latent adeno-associated virus infection elicits humoral but not cell-mediated immune responses in a nonhuman primate model. J. Virol. 73, 8549–8558.

Howard, D.B., Powers, K., Wang, Y., Harvey, B.K., 2008. Tropism and toxicity of adeno-associated viral vector serotypes 1,2,5,6,7,8,9 in rat neurons and glia in vitro. Virology 372, 24–34.

Huber, D., Petreanu, L., Ghitani, N., Ranade, S., Hromádka, T., Mainen, Z., Svoboda, K., 2008. Sparse optical microstimulation in barrel cortex drives learned behaviour in freely moving mice. Nature 451, 61–64.

Ishizuka, T., Kakuda, M., Araki, R., Yawo, H., 2006. Kinetic evaluation of photosensitivity in genetically engineered neurons expressing green algae light-gated channels. Neurosci. Res. 54, 85–94.

Jansen, V., Alvarez, L., Balbach, M., Strünker, T., Hegemann, P., Kaupp, U.B., Wachten, D., 2015. Controlling fertilization and cAMP signaling in sperm by optogenetics. Elife 4, 1–15.

Kügler, S., Kilic, E., Bähr, M., 2003. Human synapsin 1 gene promoter confers highly neuron-specific long-term transgene expression from an adenoviral vector in the adult rat brain depending on the transduced area. Gene Ther. 10, 337–347.

Karra, D., Dahm, R., 2010. Transfection techniques for neuronal cells. J. Neurosci. 30, 6171–6177.

Konermann, S., Brigham, M.D., Trevino, A.E., Hsu, P.D., Heidenreich, M., Cong, L., Platt, R.J., Scott, D.A., Church, G.M., Zhang, F., 2013. Optical control of

mammalian endogenous transcription and epigenetic states. Nature 500, 472–476.
Lange, W., Jin, L., Maybeck, V., Meisenberg, A., Baumann, A., Offenhäusser, A., 2014. Recombinant Adeno-associated virus (rAAV) –mediated transduction and optogenetic manipulation of cortical neurons in vitro. Proc. SPIE, Opt. Tech. Neurosurgery, Neurophotonics, Optogenetics 89282S.
Li, X., Gutierrez, D.V., Hanson, M.G., Han, J., Mark, M.D., Chiel, H., Hegemann, P., Landmesser, L.T., Herlitze, S., 2005. Fast noninvasive activation and inhibition of neural and network activity by vertebrate rhodopsin and green algae channelrhodopsin. Proc. Natl. Acad. Sci. U. S. A. 102, 17816–17821.
Lin, J.Y., Knutsen, P.M., Muller, A., Kleinfeld, D., Tsien, R.Y., 2013. ReaChR: a red-shifted variant of channelrhodopsin enables deep transcranial optogenetic excitation. Nat. Neurosci. 16, 1499–1508.
Madisen, L., Mao, T., Koch, H., Zhuo, J., Berenyi, A., Fujisawa, S., a, Hsu Y.-W., Garcia, A.J., Gu, X., Zanella, S., Kidney, J., Gu, H., Mao, Y., Hooks, B.M., Boyden, E.S., Buzsáki, G., Ramirez, J.M., Jones, A.R., Svoboda, K., Han, X., Turner, E.E., Zeng, H., 2012. A toolbox of Cre-dependent optogenetic transgenic mice for light-induced activation and silencing. Nat. Neurosci. 15, 793–802.
Martinez, C.Y., Hollenbeck, P.J., 2003. Transfection of primary central and peripheral nervous system neurons by electroporation. Methods Cell Biol. 71, 339–351.
Mason, M.R.J., Ehlert, E.M.E., Eggers, R., Pool, C.W., Hermening, S., Huseinovic, A., Timmermans, E., Blits, B., Verhaagen, J., 2010. Comparison of AAV serotypes for gene delivery to dorsal root ganglion neurons. Mol. Ther. 18, 715–724.
Nagel, G., Szellas, T., Huhn, W., Kateriya, S., Adeishvili, N., Berthold, P., Ollig, D., Hegemann, P., Bamberg, E., 2003. Channelrhodopsin-2, a directly light-gated cation-selective membrane channel. Proc. Natl. Acad. Sci. U. S. A. 100, 13940–13945.
Nagel, G., Brauner, M., Liewald, J.F., Adeishvili, N., Bamberg, E., Gottschalk, A., 2005a. Light activation of channelrhodopsin-2 in excitable cells of Caenorhabditis elegans triggers rapid behavioral responses. Curr. Biol. 15, 2279–2284.
Nagel, G., Szellas, T., Kateriya, S., Adeishvili, N., Hegemann, P., Bamberg, E., 2005b. Channelrhodopsins: directly light-gated cation channels. Biochem. Soc. Trans. 33, 863–866.
Nathanson, J.L., Jappelli, R., Scheeff, E.D., Manning, G., Obata, K., Brenner, S., Callaway, E.M., 2009. Short promoters in viral vectors drive selective expression in mammalian inhibitory neurons, but do not restrict activity to specific inhibitory cell-types. Front. Neural Circuits 3, 19.
Petreanu, L., Huber, D., Sobczyk, A., Svoboda, K., 2007. Channelrhodopsin-2-assisted circuit mapping of long-range callosal projections. Nat. Neurosci. 10, 663–668.
Renault, R., Sukenik, N., Descroix, S., Malaquin, L., Viovy, J.-L., Peyrin, J.-M., Bottani, S., Monceau, P., Moses, E., Vignes, M., 2015. Combining microfluidics, optogenetics and calcium imaging to study neuronal communication in vitro. PLoS One 10, e0120680.
Schultz, B.R., Chamberlain, J.S., 2008. Recombinant adeno-associated virus transduction and integration. Mol. Ther. 16, 1189–1199.
Shcherbo, D., Merzlyak, E.M., Chepurnykh, T.V., Fradkov, A.F., Ermakova, G.V., Solovieva, E.A., Lukyanov, K.A., Bogdanova, E.A., Zaraisky, A.G., Lukyanov, S., Chudakov, D.M., 2007. Bright far-red fluorescent protein for whole-body imaging. Nat. Methods 4, 741–746.
Vandendriessche, T., Thorrez, L., Acosta-Sanchez, A., Petrus, I., Wang, L., Ma, L., De Waele, L., Iwasaki, Y., Gillijns, V., Wilson, J.M., Collen, D., Chuah, M.K.L., 2007. Efficacy and safety of adeno-associated viral vectors based on serotype 8 and 9 vs. lentiviral vectors for hemophilia B gene therapy. J. Thromb. Haemost. 5, 16–24.
Wang, H., Peca, J., Matsuzaki, M., Matsuzaki, K., Noguchi, J., Qiu, L., Wang, D., Zhang, F., Boyden, E., Deisseroth, K., Kasai, H., Hall, W.C., Feng, G., Augustine, G.J., 2007. High-speed mapping of synaptic connectivity using photostimulation in Channelrhodopsin-2 transgenic mice. Proc. Natl. Acad. Sci. U. S. A. 104, 8143–8148.
Watanabe, S.Y., Albsoul-Younes, A.M., Kawano, T., Itoh, H., Kaziro, Y., Nakajima, S., Nakajima, Y., 1999. Calcium phosphate-mediated transfection of primary cultured brain neurons using GFP expression as a marker: application for single neuron electrophysiology. Neurosci. Res. 33, 71–78.
Wietek, J., Wiegert, J.S., Adeishvili, N., Schneider, F., Watanabe, H., Tsunoda, S.P., Vogt, A., Elstner, M., Oertner, T.G., Hegemann, P., 2014. Conversion of channelrhodopsin into a light-gated chloride channel. Science 344, 409–412.
Wilkinson, G.W.G., Akrigg, A., 1992. Constitutive and enhanced expression from the CMV major IE promoter in a defective adenovirus vector. Nucleic Acids Res. 20, 2233–2239.
Xiao, X., Li, J., Samulski, R.J., 1998. Production of high-titer recombinant adeno-associated virus vectors in the absence of helper adenovirus. J. Virol. 72, 2224–2232.
Ye, H., Baba, M.D.-E., Peng, R.-W., Fussenegger, M., 2011. A synthetic optogenetic transcription device enhances blood-glucose homeostasis in mice. Science 332, 1565–1568.
Yizhar, O., Fenno, L.E., Prigge, M., Schneider, F., Davidson, T.J., O'shea, D.J., Sohal, V.S., Goshen, I., Finkelstein, J., Paz, J.T., Stehfest, K., Fudim, R., Ramakrishnan, C., Huguenard, J.R., Hegemann, P., Deisseroth, K., 2011. Neocortical excitation/inhibition balance in information processing and social dysfunction. Nature.
Zeitelhofer, M., Vessey, J.P., Thomas, S., Kiebler, M., Dahm, R., 2009. Transfection of cultured primary neurons via nucleofection. In: Current Protocols in Neuroscience. John Wiley & Sons, Inc.
Zhang, F., Wang, L.-P., Boyden, E.S., Deisseroth, K., 2006. Channelrhodopsin-2 and optical control of excitable cells. Nat. Methods 3, 785–792.
Zhu, G., Du, L., Jin, L., Offenhäusser, A., 2016. Effects of morphology constraint on electrophysiological properties of cortical neurons. Sci. Rep. 6, 23086.